Frontiers in Bioscience Landmark

Front. Biosci. (Landmark Ed) **2023**; 28(3): 45
https://doi.org/10.31083/j.fbl2803045

Original Research

Astragaloside IV Inhibits NLRP3 Inflammasome-Mediated Pyroptosis via Activation of Nrf-2/HO-1 Signaling Pathway and Protects against Doxorubicin-Induced Cardiac Dysfunction

Xueheng Chen[1,2], Chao Tian[1,2], Zhiqiang Zhang[1,2], Yiran Qin[3], Runqi Meng[1,2], Xuening Dai[1,2], Yuanyuan Zhong[1,2], Xiqing Wei[1,2], Jinguo Zhang[1,2,*], Cheng Shen[1,2,*]

[1]Affiliated Hospital of Jining Medical University, Clinical Medical College, Jining Medical University, 272000 Jining, Shandong, China
[2]Jining Key Laboratory for Diagnosis and Treatment of Cardiovascular Diseases, 272000 Jining, Shandong, China
[3]Cheeloo College of Medicine, Shandong University, 250012 Jinan, Shandong, China
*Correspondence: zhangjinguo@mail.jnmc.edu.cn (Jinguo Zhang); shencheng1117@126.com (Cheng Shen)
Academic Editor: Ioanna-Katerina Aggeli
Submitted: 19 October 2022 Revised: 13 December 2022 Accepted: 14 December 2022 Published: 3 March 2023

Abstract

Background: Doxorubicin (DOX) is an effective broad-spectrum antitumor drug, but its clinical application is limited due to the side effects of cardiac damage. Astragaloside IV (AS-IV) is a significant active component of *Astragalus membranaceus* that exerts cardioprotective effects through various pathways. However, whether AS-IV exerts protective effects against DOX-induced myocardial injury by regulating the pyroptosis is still unknown and is investigated in this study. **Methods**: The myocardial injury model was constructed by intraperitoneal injection of DOX, and AS-IV was administered via oral gavage to explore its specific protective mechanism. Cardiac function and cardiac injury indicators, including lactate dehydrogenase (LDH), cardiac troponin I (cTnI), creatine kinase isoenzyme (CK-MB), and brain natriuretic peptide (BNP), and histopathology of the cardiomyocytes were assessed 4 weeks post DOX challenge. Serum levels of IL-1β, IL-18, superoxide dismutase (SOD), malondialdehyde (MDA) and glutathione (GSH) and the expression of pyroptosis and signaling proteins were also determined. **Results**: Cardiac dysfunction was observed after the DOX challenge, as evidenced by reduced ejection fraction, increased myocardial fibrosis, and increased BNP, LDH, cTnI, and CK-MB levels ($p < 0.05$, N = 3–10). AS-IV attenuated DOX-induced myocardial injury. The mitochondrial morphology and structure were also significantly damaged after DOX treatment, and these changes were restored after AS-IV treatment. DOX induced an increase in the serum levels of IL-1β, IL-18, SOD, MDA and GSH as well as an increase in the expression of pyroptosis-related proteins ($p < 0.05$, N = 3–6). Besides, AS-IV depressed myocardial inflammatory-related pyroptosis via activation of the expressions of nuclear factor E2-related factor 2 (Nrf-2) and heme oxygenase 1 (HO-1) ($p < 0.05$, N = 3). **Conclusions**: Our results showed that AS-IV had a significant protective effect against DOX-induced myocardial injury, which may be associated with the activation of Nrf-2/HO-1 to inhibit pyroptosis.

Keywords: *Astragalus membranaceus*; doxorubicin; pyroptosis; Nrf-2/HO-1; cardiac dysfunction; cardioprotection

1. Introduction

Doxorubicin (DOX) is an effective antitumor drug that is used to treat a variety of cancers, including solid organ tumors and hematologic malignancies [1–4]. DOX kills cancer cells mainly through the inhibition of DNA synthesis, interference with topoisomerase II activity, and induction of oxidative stress [5–7]. However, despite its antitumor effects, DOX is associated with causing undesired cell death in healthy tissues and cells [8,9]. The side effects of DOX, particularly its dose-dependent cardiotoxicity, can lead to heart failure, which greatly limits its clinical application [10]. In the past decades, multiple studies have clarified the pathogenesis of DOX-induced cardiac dysfunction, especially cell death, which plays an important role in DOX-induced myocardial injury, including autophagy, apoptosis, and necrosis [11,12]. In recent years, it has been reported that pyroptosis is involved in cardiomyocyte death and cardiac dysfunction induced by DOX. However, its underlying regulatory mechanism has not been fully investigated [13]. Therefore, further exploration of the specific mechanisms by which DOX causes cardiomyocyte death could help to mitigate its cardiotoxic effects.

Pyroptosis is caspase-dependent inflammatory programmed cell death with inflammasome activation being a key process in the development of pyroptosis [14]. Among these, nod-like receptor protein 3 (NLRP3) inflammasome-mediated pyroptosis is the most important pathway involved in the pathogenesis of cardiovascular diseases [15]. NLRP3 can be activated by external stimuli and interact with apoptosis-associated speck-like protein (ASC). After activation by NLRP3, ASC recruits cysteine protease caspase-1 (pro-caspase-1) to form the NLRP3 inflammasome, which leads to the activation of caspase-1 to form cleaved caspase-1 [16]. Subsequently, cleaved caspase-1 cleaves full length gasdermin D (GSDMD-FL) to produce an N-terminal activated product (GSDMD-N), leading to the conversion of IL-1β and IL-18 precursors into

mature inflammatory factors. GSDMD-N mediates the formation of cell membrane pores, leading to cell swelling, cell membrane rupture, and release of inflammatory factors, resulting in pyroptosis. Recent studies have demonstrated that pyroptosis causes DOX-induced myocardial injury [13,17,18]. Besides, it has also been shown to induce myocardial pyroptosis via the NLRP3-caspase-1 pathway [19]. Identifying drugs that can inhibit NLRP3-mediated pyroptosis may effectively alleviate DOX-induced cardiac damage.

Although some drugs, such as dexrazoxane, can be used as cardioprotective agents and have been found to reduce DOX-induced myocardial damage. However, they have a potential risk of secondary malignancies [20]. Additionally, some traditional drugs for heart disease, such as angiotensin-converting enzyme inhibitors and beta-blockers, have not been clearly proven to protect against DOX-induced myocardial injury, and these drugs also have also been reported to exhibit adverse effects [20]; hence it is necessary to explore drugs with few side effects to improve DOX-induced cardiotoxicity. Compared with traditional compound drugs, natural drugs have the advantages of fewer adverse effects, less long-term toxicity, and variable bioavailability [21]. Modern research has found that herbal medicines exert a polypharmacological action and can effectively prevent and treat cardiovascular diseases [22]. *Astragalus membranaceus* is a traditional Chinese herbal medicine which is widely used in the treatment of cardiovascular diseases due to its effects of invigorating and promoting yang, diffusing edema, and detoxifying muscles [23]. AS-IV is a key active ingredient extracted from *Astragalus membranaceus* and is involved in various pharmacological properties including antioxidant activity, inhibition of apoptosis, inhibition of fibrosis, and immune modulation [24]. Among these, its cardioprotective effects are the most important. It has been reported that AS-IV alleviates heart failure by improving myocardial energy metabolism [25,26]. Our previous studies also suggested that AS-IV has a protective effect against myocardial fibrosis and reverse ventricular hypertrophy [27]. Currently, new studies have found that AS-IV has significant anti-inflammatory effects [28,29]. AS-IV attenuates pulmonary toxicity and cerebral ischemia-reperfusion injury by inhibiting NLRP3 inflammasome-mediated pyroptosis. However, there is a paucity of knowledge as to whether AS-IV protects cardiac function by inhibiting pyroptosis of cardiomyocytes. Considering that there is no specific drug for DOX-induced myocardial injury, this study explores whether AS-IV, a traditional Chinese medicine with low side effects, has a good curative effect, and aims to investigate its possible mechanism and regulatory pathway.

2. Materials and Methods

2.1 Animal Model

Specific pathogen free (SPF) healthy male C57BL/6 mice (n = 40, weight 22 ± 2 g, 8–10 weeks) were purchased from Jinan Pengyue Experimental Animal Breeding Co., Ltd. (Jinan, China). The experiments were conducted in accordance with the principles approved by the Animal Care and Use Committee of the Affiliated Hospital of Jining Medical University (Permission number: 2021C104). All animal procedures conformed to the US of Health Guidelines for the Care and Use of Laboratory Animals. Mice were kept in a temperature- and humidity-controlled environment (22 ± 2 °C and 12 h dark/light schedule) with free access to chow and water. One week after acclimation, the mice were divided into four groups (N = 10 per group) using a random number table method. According to published articles and our preliminary experiments [30], mice in the DOX-treated group were intraperitoneally injected with DOX at 2 mg/kg every alternate day with a cumulative dosage of 28 mg/kg. Mice in the control group (CON) received an intraperitoneal injection of an equivalent volume of saline. The AS-IV treatment groups were intragastrically administered 40 mg/kg AS-IV (dissolved in saline) daily for 4 weeks after the first injection of DOX, according to previous experiments [31]. The AS-IV group was given only the same dose of AS-IV to eliminate the effect of AS-IV alone on the results. Mice were sacrificed by over-anesthesia with 100 mg/kg sodium pentobarbital (P3761, Sigma-Aldrich (Shanghai) Trading Co.Ltd., Shanghai, China) after 4 weeks. The bodyweight of the mice was recorded, and blood was obtained from the carotid artery of mice. DOX (D8740) was purchased from Solarbio Science & Technology Co., Ltd. (Beijing, China), and AS-IV (T2973) was purchased from TOPSCIENCE Biotech Co., Ltd. (Shanghai, China). The purity of DOX was 99%, and the purity of ASIV was 99.29%.

2.2 Echocardiographic Assessment

The cardiac function of mice was assessed after 4 weeks. Mice from the four groups were anesthetized with 1–2% isoflurane (1349003, Sigma-Aldrich (Shanghai) Trading Co.Ltd., Shanghai, China), and transthoracic echocardiography was performed using an animal-specific ultrasound imaging system with a 40 MHz transducer (M9Vet, Mindray, Shenzhen, China). Mice were placed supine and fixed on a board, the parasternal long axis was taken, and M-mode images were obtained at the inferior border of the mitral papillary muscle. Left ventricular ejection fraction (LVEF), left ventricular fractional shortening (LVFS), left ventricular internal dimension at end-diastole (LVIDd), and left ventricular internal dimension at end-systole (LVIDs) were measured and calculated to evaluate cardiac function.

2.3 Serum Enzyme-Linked Immunosorbent Assay (ELISA)

Blood samples were collected from the carotid artery after over-anesthesia. Serum was obtained after centrifugation of whole blood. According to the instructions of each kit, ELISA was performed to detect the serum concentration of the heart failure marker brain natriuretic peptide (BNP, E-EL-M0204c, Elabscience Biotechnology Co., Ltd., Wuhan, China), the myocardial injury markers lactate dehydrogenase (LDH, 12239, MEIMIAN Industrial Co., Ltd., Yancheng, China), creatine kinase isoenzyme (CK-MB, E-EL-M0355c, Elabscience Biotechnology Co., Ltd., Wuhan, China), cardiac troponin I (cTnI, E-EL-M1203c, Elabscience Biotechnology Co., Ltd., Wuhan, China), the inflammatory markers IL-1β (ab197742, Abcam, Cambridge, UK) and IL-18 (ab216165, Abcam, Cambridge, UK), and the oxidative stress markers superoxide dismutase (SOD, JL12237, j&l Biological, Shanghai, China), malondialdehyde (MDA, JL13329, j&l Biological, Shanghai, China), and glutathione (GSH, JL20360, j&l Biological, Shanghai, China). Absorbance was measured at 450 nm using a microplate reader (BioTek Cytation 5, American Berten Instrument Co., Ltd., Santa Clara, CA, US).

2.4 Histological Staining

Mice were sacrificed after 4 weeks of DOX and AS-IV treatment. The heart of each mouse was removed and the weight was recorded. Cardiac tissue was rinsed with phosphate-buffered saline (PBS), fixed with 4% paraformaldehyde for at least 48 h, and embedded in paraffin. The slices were cut into 5 μm sections and stained with HE, Masson's trichrome, and wheat germ agglutinin (WGA) as previously described [31,32]. Five random fields of cardiac tissue were imaged using a microscope (Nikon Eclipse E100, Nikon, Tokyo, Japan). ImageJ software version 1.8.0 (National Institutes of Health, Bethesda, MD, USA) was used to evaluate myocardial fibrosis and the cross-sectional areas of the cardiomyocytes ($\geq$2 random areas in $\geq$3 mice/group).

2.5 Transmission Electron Microscope (TEM)

Fresh myocardial tissue was dissected into small pieces of approximately 1 mm^3 and fixed in 2.5% glutaraldehyde (pH 7.4) for 2 h at room temperature (RT). After rinsing with PBS, the tissues were then fixed in 1% osmic acid at 4 °C for 2 h. The samples were then dehydrated in gradient ethanol and embedded in Epon-Araldite resin. Ultrathin sections were prepared and collected for microstructure analysis and then observed using a HITACHI transmission electron microscope.

2.6 Immunohistochemical Analysis

To determine the expression of NLRP3, caspase-1, and GSDMD in the heart, immunohistochemical analysis was performed using anti-NLRP3 (GB11300, Servicebio, Wuha, China), anti-caspase-1 (sc-56036, Santa Cruz, Dallas, TX, USA), and anti-GSDMD (sc-81868, Santa Cruz, Dallas, TX, USA) antibodies as previously described [33]. Briefly, after dewaxing and antigen repair, the paraffin sections were placed in 3% hydrogen peroxide for 25 min at RT. The sections were subsequently incubated with primary antibodies overnight (16–18 h) at 4 °C and secondary antibodies at RT for 50 min. The sections were stained with diaminobenzidine (G1211, Servicebio, Wuha, China) and hematoxylin (G1004, Servicebio, Wuha, China). After sufficient drying, the slides were photographed and evaluated using the ImageJ software.

2.7 Western Blot Analysis

Heart tissues were fully dissolved in RIPA buffer (P0013B, Beyotime, Shanghai, China) containing protease inhibitor (P1045, Beyotime, Shanghai, China) and phosphatase inhibitor (P1045, Beyotime, Shanghai, China). After examination of protein concentrations using a BCA kit (P0010, Beyotime, Shanghai, China), 30 μg of protein samples were separated using 12.5% or 10% sodium dodecyl sulfate-polyacrylamide gel electrophoresis and transferred to polyvinylidene fluoride membranes. After blocking with protein-free rapid blocking solution (1$\times$) at RT for 30 min, the membranes were incubated with primary antibodies at 4 °C overnight. The primary antibodies used were NLRP3 (ab263899, Abcam, Cambridge, UK), ASC (#67824, CST, Boston, MA, USA), caspase-1 (A0964, ABclonal, Wuhan, China), GSDMD (ab219800, Abcam, Cambridge, UK), GSDMD-N (#10137, CST, Boston, MA, USA), cleaved caspase-1 (#89332, CST, Boston, MA, USA), IL-1β (ab283818, Abcam, Cambridge, UK), IL-18 (ab191860, Abcam, Cambridge, UK), Nrf-2 (A1244, ABclonal, Wuhan, China), pNrf-2 (#DF7519, Affinity Biosciences, Jiangsu, China), HO-1 (#82206, CST, Boston, MA, USA), and β-actin (#4970, CST, Boston, MA, USA). The bands were visualized using a sensitive ECL chemiluminescence kit (PK10002, Proteintech, Chicago, IL, USA) after incubation with horseradish peroxidase-conjugated secondary antibody (AS014, ABclonal, Wuhan, China) at RT for 2 h. Images were obtained using the ChemiDoc system (Tanon 5800, Shanghai Tanon Technology Co., Ltd., Shanghai, China), and quantitative analysis of the blots was conducted using ImageJ software with β-actin as the loading control.

2.8 Statistical Analysis

All data are expressed as the mean $\pm$ standard error of the mean (SEM). One-way analysis of variance followed by Tukey post-hoc test (homogeneous variance) or Dunnett T3 post-hoc test (Unequal variances) was performed using SPSS 26 (SPSS Inc., Chicago, IL, USA) and GraphPad Prism version 9.0 (GraphPad Software LLC, San Diego, CA, USA). Statistical significance was set at $p < 0.05$.

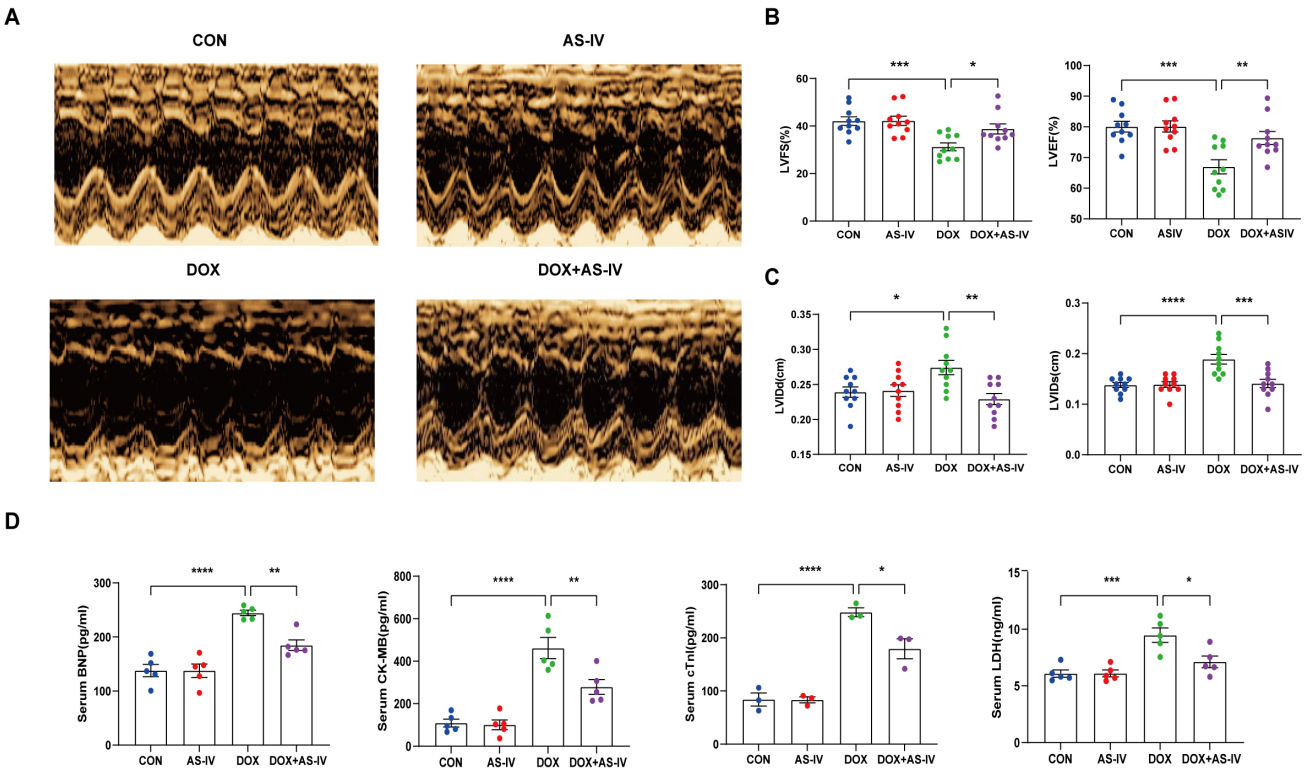

Fig. 1. AS-IV attenuates DOX-induced cardiac dysfunction. (A) Representative M-mode images of echocardiograms of experimental animals in each group. (B) Quantitative analysis of left ventricular fractional shortening (LVFS) and left ventricular ejection fraction (LVEF). (C) Quantitative analysis of left ventricular internal dimension at end-diastole (LVIDd) and left ventricular internal dimension at end-systole (LVIDs). (D) Quantitative analysis of serum concentration of brain natriuretic peptide (BNP), creatine kinase isoenzyme (CK-MB), cardiac troponin I (cTnI) and lactate dehydrogenase (LDH). CON, mice treated with an equal volume of saline. AS-IV, mice treated with 40 mg/kg AS-IV. DOX, mice treated with 2 mg/kg BW doxorubicin every other day with a cumulative dosage of 28 mg/kg. DOX + AS-IV, mice treated with doxorubicin and AS-IV. Data are shown as mean ± SEM, N = 3–10, * $p < 0.05$, ** $p < 0.01$, *** $p < 0.001$, **** $p < 0.0001$. Using Shapiro-Wilk test to test the normality of the distribution, all the data are in accordance with the normal distribution. All the data were compared by one-way analysis of variance followed by Tukey post-hoc test for multiple comparisons.

3. Results

3.1 AS-IV Improves DOX-Induced Cardiac Dysfunction

To investigate the cardioprotective effects of AS-IV, DOX-treated mice were subsequently treated with AS-IV. After 4 weeks of intervention, transthoracic echocardiography was performed to evaluate cardiac structure and function in the four groups of mice (Fig. 1A). Our data indicated that intraperitoneal injection of DOX caused cardiac dysfunction, as evidenced by reduced LVEF and LVFS, compared with that in the control group. However, LVEF and LVFS significantly improved in mice treated with AS-IV (Fig. 1B). In terms of heart structure, LVIDd and LVIDs were increased in the DOX group compared to the control group, and LVIDd and LVIDs were lower in the AS-IV-treated mice than in the DOX-treated mice (Fig. 1C). To further evaluate the effects of DOX and AS-IV on cardiac function, we measured serum BNP, CK-MB, cTnI, and LDH levels, which are classical biomarkers of cardiac injury. As shown in Fig. 1D, the serum levels of BNP, CK-MB, cTnI, and LDH of the mice in the DOX group were significantly higher than those in the control group. Compared with the model group, the serum concentrations of these heart injury markers were reduced in the AS-IV-treated group. The results indicate that AS-IV alone does not alter cardiac function but can improve DOX-induced cardiac dysfunction.

3.2 AS-IV Attenuates DOX-Induced Myocardial Fibrosis and Mitochondrial Injuries

Histological examinations were then performed to examine the microstructural abnormalities of mice in the four groups. HE staining showed that myocardial fibers in the control group were neatly and tightly arranged, with distinct nuclei, while myocardial tissue in the DOX group was disorganized. However, treatment with AS-IV effectively improved the histopathological features of the myocardial tissue (Fig. 2A). Masson-stained collagen was significantly increased in the DOX group compared to that in the other groups (Fig. 2B). In addition, WGA staining showed that

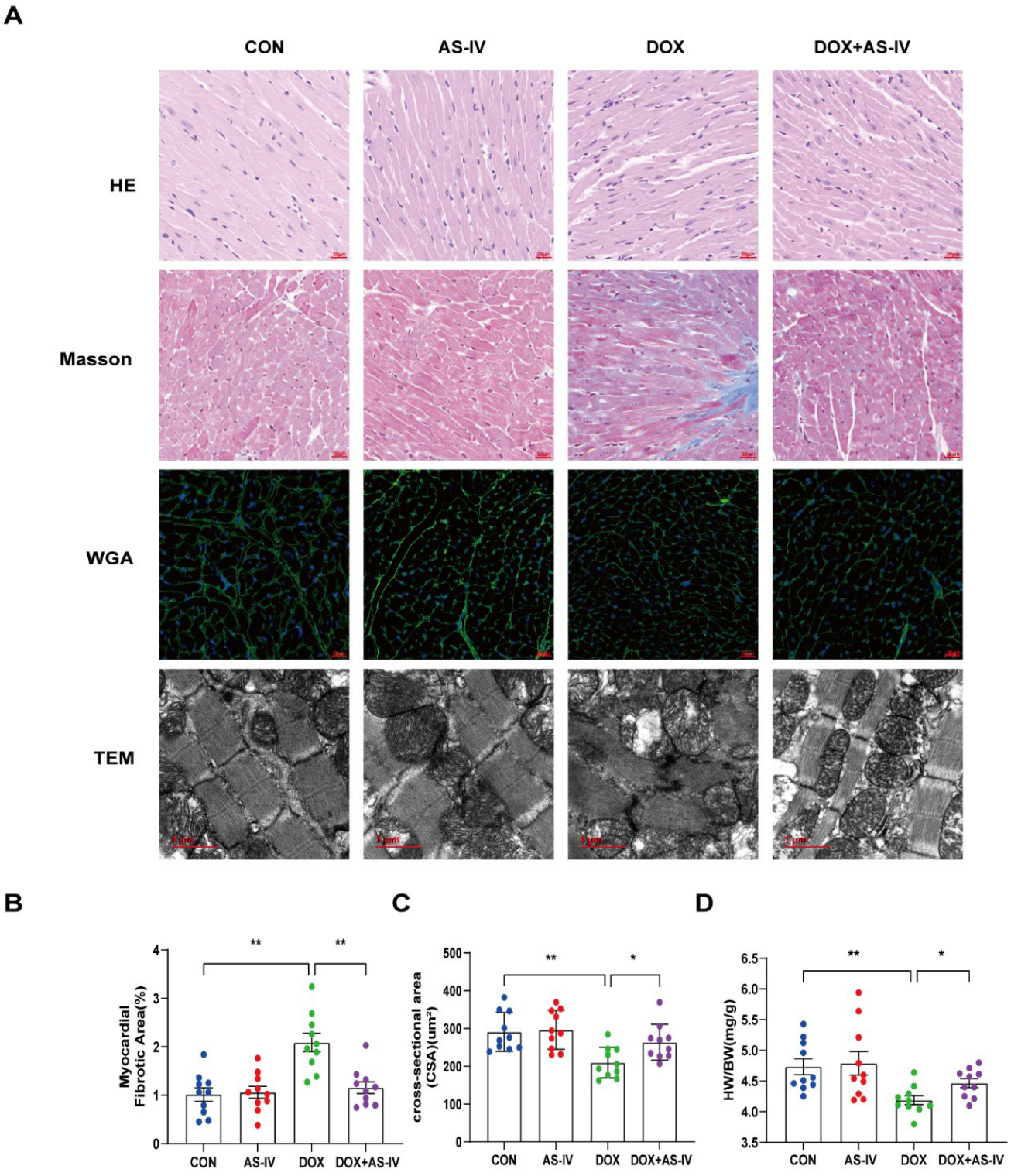

Fig. 2. AS-IV ameliorated DOX-induced myocardial remodeling and myocardial injuries. (A) Representative images of HE (magnification, 400×), Masson (magnification, 400×), WGA (magnification, 400×), and transmission electron microscopy (TEM) images of the four groups (magnification, 15,000×). (B,C) Quantitative analysis of myocardial fibrosis area and the cross-sectional area of myocardial cells. (D) the ratio of heart weight to body weight (HW/BW). N = 10, data are shown as mean ± SEM; * $p < 0.05$, ** $p < 0.01$. Using Shapiro-Wilk test to test the normality of the distribution, all the data are in accordance with the normal distribution. Myocardial fibrosis area and HW/BW were compared by one-way analysis of variance followed by Dunnett T3 post-hoc test for multiple comparisons and cross-sectional area (CSA) followed by Tukey post-hoc test.

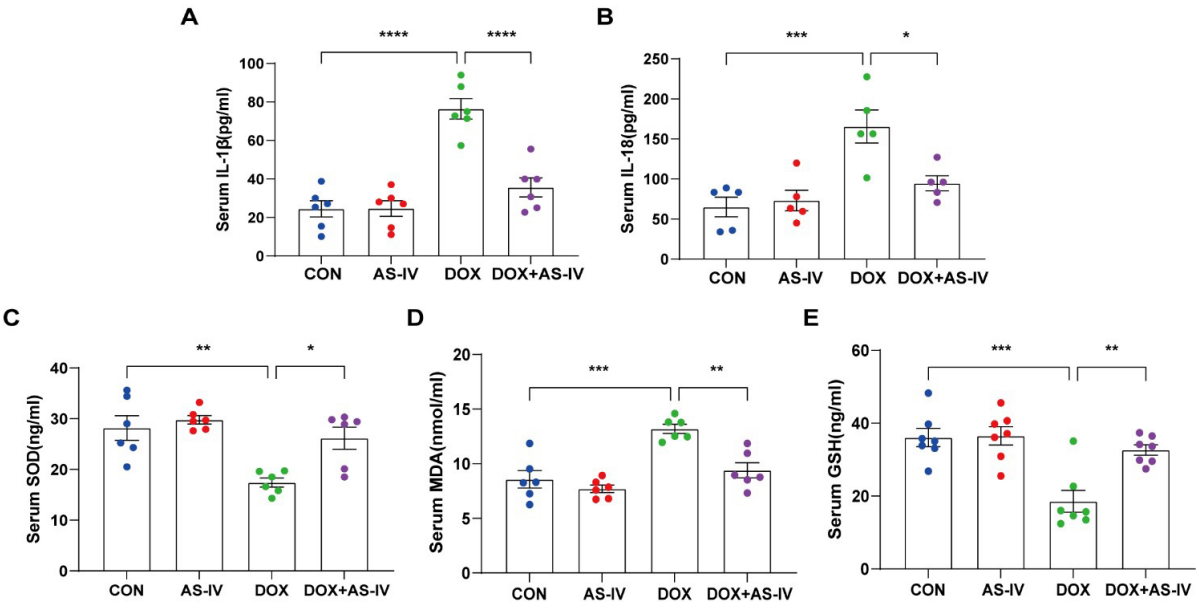

Fig. 3. AS-IV ameliorated the release of DOX-induced serum inflammatory factors and oxidative stress levels. (A–E) Quantitative analysis of serum concentration of IL-1β, IL-18, SOD, MDA and GSH. N = 5–7, data are shown as mean $\pm$ SEM; * $p < 0.05$, ** $p < 0.01$, *** $p < 0.001$, **** $p < 0.0001$. Using Shapiro-Wilk test to test the normality of the distribution, all the data are in accordance with the normal distribution. All the data were compared by one-way analysis of variance followed by Tukey post-hoc test for multiple comparisons.

the mean area of cardiomyocytes in the DOX-induced myocardial injury group was significantly lower than that in the control group, and AS-IV treatment increased the area of cardiomyocytes (Fig. 2C), which was consistent with the ratio of heart weight to body weight (HW/BW) (Fig. 2D). TEM was conducted to further detect the effects of DOX and AS-IV on the ultrastructure of the cardiomyocytes. In the absence of DOX, mitochondria were arranged normally in organized sarcomeres. However, in the DOX-treated group, mitochondrial damage was observed and was characterized by swelling and vacuolization as well as disarrangement of myofilaments, the disappearance of the H-band, reduced ridge lysis, and widened Z-rays. Fewer injuries were observed after AS-IV administration (Fig. 2A). These results demonstrate that AS-IV attenuates myocardial fibrosis and mitochondrial damage.

3.3 AS-IV Attenuates DOX-Induced Inflammation and Oxidative Stress

As the activation of inflammasomes and release of inflammatory factors are important in the process of pyroptosis and the fact that oxidative stress can cause pyroptosis [34], we measured the levels of serum IL-1β, IL-18, SOD, GSH and MDA. The results showed that administration of DOX increased the serum levels of IL-1β, IL-18, MDA and decreased the serum levels of SOD and GSH compared to that in the control group, while AS-IV treatment decreased serum IL-1β, IL-18, MDA and increased SOD and GSH levels (Fig. 3A–E). In addition, treatment with AS-IV alone did not alter the levels of serum inflammatory factors and oxidative stress indicators. The results showed that DOX increases the release of inflammatory factors and the level of oxidative stress, whereas AS-IV treatment reduces the levels of the inflammatory and oxidative stress markers.

3.4 AS-IV Attenuates DOX-Induced Myocardial Injury by Inhibiting NLRP3 Inflammasome-Mediated Myocardial Pyroptosis in Mice

To further investigate whether AS-IV alleviates myocardial injury by inhibiting DOX-induced myocardial pyroptosis, we first examined the expression of pyroptosis-related proteins in myocardial tissue using immunohistochemistry (Fig. 4A). Quantitative immunohistochemical analysis showed that the expression of pyroptosis-related proteins NLRP3, caspase-1, and GSDMD dramatically increased after DOX treatment, and subsequent treatment with AS-IV markedly attenuated the expression of these markers (Fig. 4B–D). In addition, the protective role of AS-IV was confirmed using immunoblotting (Fig. 5A). As shown in Fig. 5B,C, DOX significantly upregulated the expression of NLRP3 and ASC and activated the cleavage of caspase-1, GSDMD-FL, IL-1β, and IL-18. Treatment with only AS-IV did not affect myocardial pyroptosis; however, it rescued DOX-induced activation of pyroptosis. The remaining two western blots images can be found in the supplemental file.

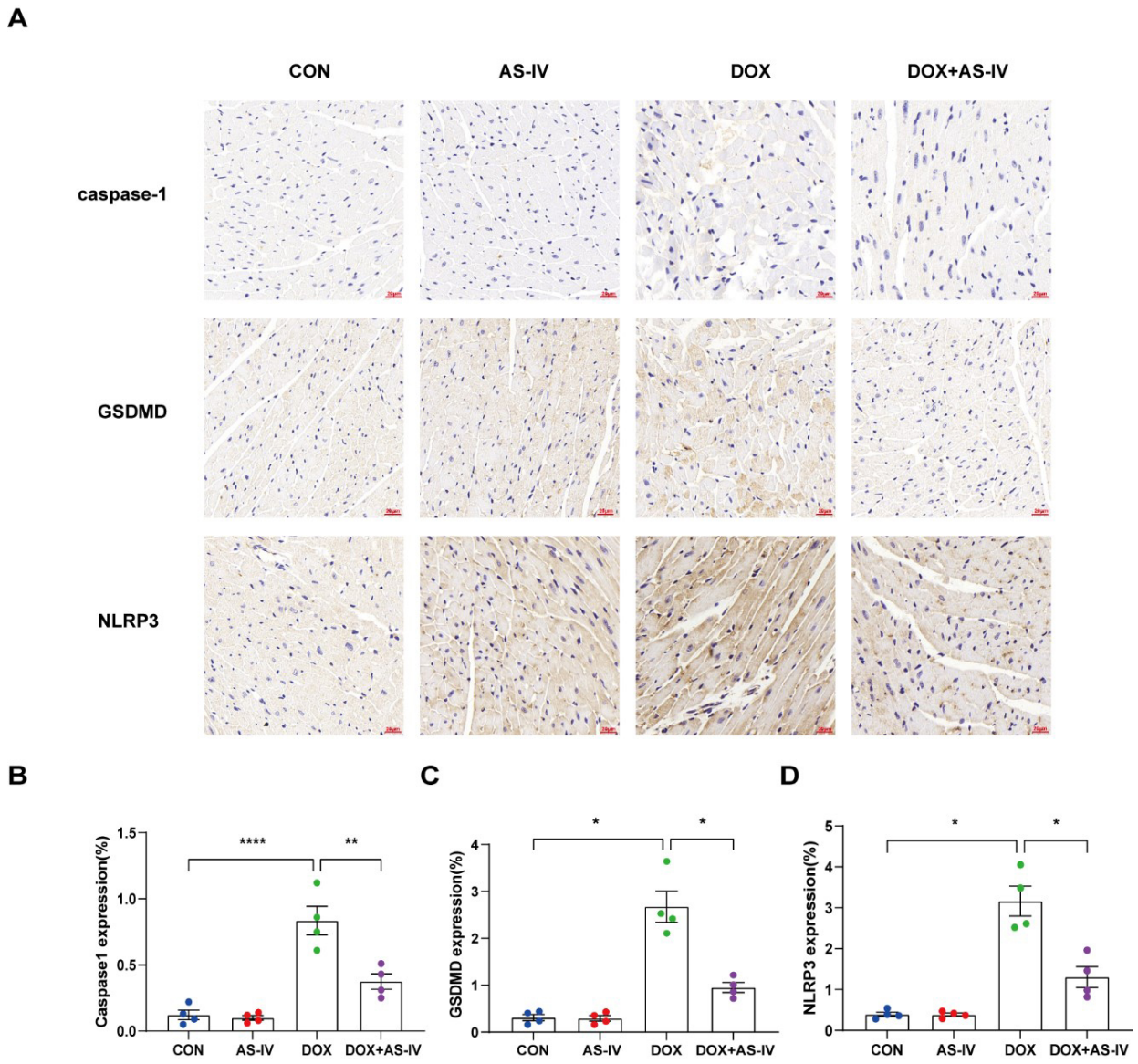

Fig. 4. AS-IV attenuates the expression of pyroptosis proteins in myocardial tissue. (A) Representative immunohistochemical images of the four groups. (B–D) Quantitative analysis of caspase-1, GSDMD and NLRP3. N = 4, data are shown as mean ± SEM, * $p < 0.05$, ** $p < 0.01$, **** $p < 0.0001$. Using Shapiro-Wilk test to test the normality of the distribution, all the data are in accordance with the normal distribution. All the data were compared by one-way analysis of variance followed by Tukey post-hoc test for multiple comparisons.

3.5 AS-IV Rescues DOX-Induced Inhibition Nrf-2/HO-1 Pathway

The Nrf-2 signaling pathway has been found to have a potential protective effect on neuronal, vascular endothelial, and cardiac myocyte injury caused by pyroptosis [35–37]. To further explore the possible regulatory pathways of pyroptosis, we examined the expression of Nrf-2, pNrf-2 and HO-1 (Fig. 6A). Western blotting results in Fig. 6 reveal a reduced expression of Nrf-2, pNrf-2, and HO-1 in the DOX-treated group. AS-IV activates Nrf-2 to phosphorylate it and increases the expression of HO-1. The remaining two western blots images can be found in the supplemental file.

4. Discussion

Our findings establish that AS-IV activates the Nrf-2/HO-1 signaling pathway and inhibits cardiomyocyte pyroptosis, and highlights the protective effect of AS-IV against DOX-induced myocardial injury. First, we confirmed the cardiotoxic effects of DOX, as evidenced by the reduced ejection fraction, increased myocardial fibrosis, and elevated serum markers of cardiac injury. Second, we demonstrated that AS-IV restored the deleterious effects of DOX by inhibiting NLRP3-related pyroptosis. Third, we found the activated Nrf-2/HO-1 pathway to be the potential mechanism underlying the protective effects of AS-IV in reducing DOX-induced cardiotoxicity. These findings in-

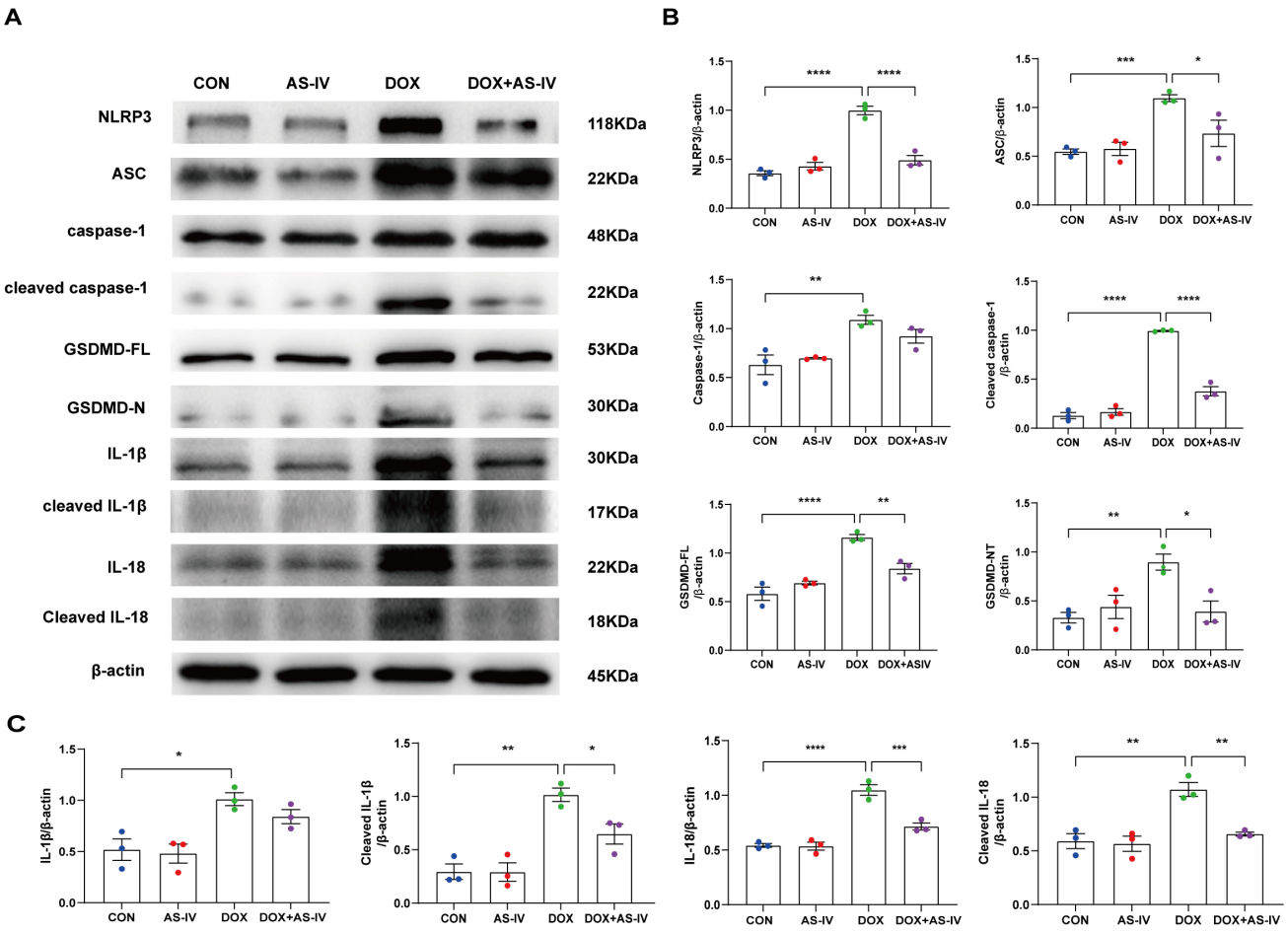

Fig. 5. AS-IV inhibits the expression of DOX-induced pyroptosis-associated proteins. (A) Representative images of western blot from cardiac tissue following DOX and AS-IV treatments. (B,C) Quantitative analysis of NLRP3, ASC, caspase-1, cleaved caspase-1, GSDMD-FL (full length gasdermin D), GSDMD-N (activated gsdmd), IL-1β, cleaved IL-1β, IL-18 and cleaved IL-18. N = 3, data are shown as mean $\pm$ SEM, * $p < 0.05$, ** $p < 0.01$, *** $p < 0.001$, **** $p < 0.0001$. Using Shapiro-Wilk test to test the normality of the distribution, all the data are in accordance with the normal distribution. All the data were compared by one-way analysis of variance followed by Tukey post-hoc test for multiple comparisons.

dicate the potential therapeutic implication of AS-IV in inhibiting pyroptosis and ameliorating DOX-related cardiac complications.

DOX is a widely used anti-cancer drug but has limited clinical applications due to its deleterious effect on multiple organs, particularly the heart. Previous studies have shown that oxidative stress and apoptosis are involved in DOX-induced cardiomyopathy [38–40]. Moreover, excessive inflammatory responses have been demonstrated to play vital roles in DOX-induced multiple organ damage, and inhibition of the inflammatory response could potentially alleviate the possibility of organ injuries [41,42]. Inflammasomes are polyprotein complexes that induce both inflammation and pyroptosis. Studies have provided insights into the activation and regulation of inflammasome complexes, including NLRP1, NLRP3, NLR family CARD domain-containing 4 (NLRC4), and pyrin [43]. Recent evidence has demonstrated that DOX can cause cardiotoxicity by activating NLRP1 inflammasome-induced pyroptosis [44]. It has also been shown that NLRP3 inflammasome-mediated pyroptosis plays an important role in the pathogenesis of DOX-induced non-ischemic dilated cardiomyopathy, and inhibition of the NLRP3 inflammasome significantly attenuates DOX-induced cardiotoxicity in mice [17,45]. Our study also showed that DOX increases myocardial NLRP3 inflammasome-associated pyroptosis and inflammation, as evidenced by the increased expression of related proteins. These studies confirm that inflammation-related pyroptosis is a key pathogenic mechanism of DOX-induced cardiotoxicity.

Radix astragali (RA), a traditional Chinese medicinal herb, is widely used in the treatment of cardiovascular, respiratory, and liver diseases as well as immune disorders [46]. Huangqi injection is derived from RA and is widely used in the clinical treatment of patients with chronic heart failure [47,48]. Astragalus polysaccharide, another extract

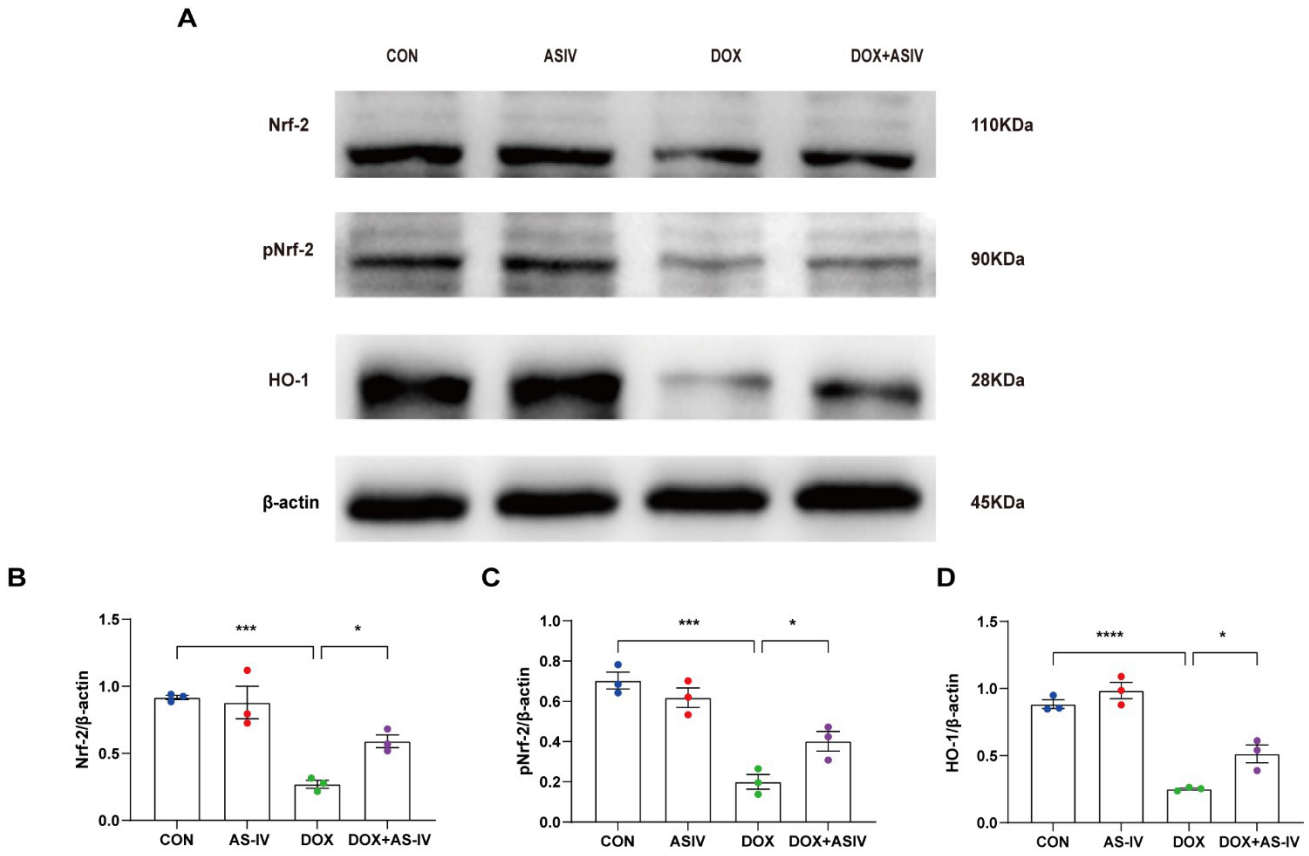

Fig. 6. AS-IV inhibits DOX-induced pyroptosis by activating the Nrf-2/HO-1 signaling pathway. (A) Representative images of western blot analysis of cardiac tissue following DOX and AS-IV treatments. (B–D) Quantitative analysis of Nrf-2, pNrf-2 and HO-1. N = 3, data are shown as mean ± SEM, * $p < 0.05$, *** $p < 0.001$, **** $p < 0.0001$. Using Shapiro-Wilk test to test the normality of the distribution, all the data are in accordance with the normal distribution. All the data were compared by one-way analysis of variance followed by Tukey post-hoc test for multiple comparisons.

of RA, has been shown to improve the quality of life of cancer patients and reduce side effects [49,50]. AS-IV is the most critical active ingredient of RA. In the Chinese Pharmacopoeia, AS-IV is used as a quality control indicator for RA, whereas the European Pharmacopoeia also specifically considered using AS-IV for testing the quality of RA [51]. Previous studies have shown that AS-IV reduces endothelial damage and cardiac dysfunction induced by elevated levels of blood glucose, lipids, inflammatory markers, and reactive oxygen species (ROS) by inhibiting oxidative stress, inflammatory responses, and apoptosis [52–55]. Consistently, we also found that AS-IV increased the ejection fraction, reversed ventricular remodeling, and improved cardiac function in mice after the DOX challenge. Moreover, it has been found that AS-IV attenuates cerebral ischemia-reperfusion injury and PM2.5-induced pulmonary toxicity by inhibiting pyroptosis [56–58], suggesting its role in regulating pyroptosis. Therefore, we investigated the role and mechanisms underlying pyroptosis, stimulated by AS-IV, in protecting against DOX-induced myocardial injuries. Notably, this study found that AS-IV inhibits the expression of NLRP3 inflammasome-related pyroptotic proteins after the DOX challenge. The present study further clarifies the role and mechanisms by which AS-IV ameliorates DOX-induced myocardial injury by attenuating myocardial pyroptosis.

ROS has been found to play an important role in NLRP3 inflammasome activation [59–61]. Oxidative stress, as the upstream signal of NLRP3 inflammasome activation, can up-regulate the expression of NLRP3, procaspase-1, and ASC and promote the assembly of the NLRP3 inflammasome, which in turn causes pyroptosis [34]. Nrf-2 is an important redox transcription factor that can improve the oxidative stress status of the body and maintain the redox balance of cells by regulating the production of antioxidant enzymes [62]. Phosphorylation of Nrf2 has been shown to play a key role in antioxidant stress, inhibiting the activation of NLRP3 inflammasome [63,64]. HO-1 is regulated by Nrf-2 and is the rate-limiting step that catalyzes the oxidative degradation of heme, during which it is converted to bilirubin, and plays a key role in inflammation [65]. Moreover, it was found that the activation of Nrf-2 could attenuate the classical pyroptosis pathway involved in oxidative stress [37,66]. Our previous study also

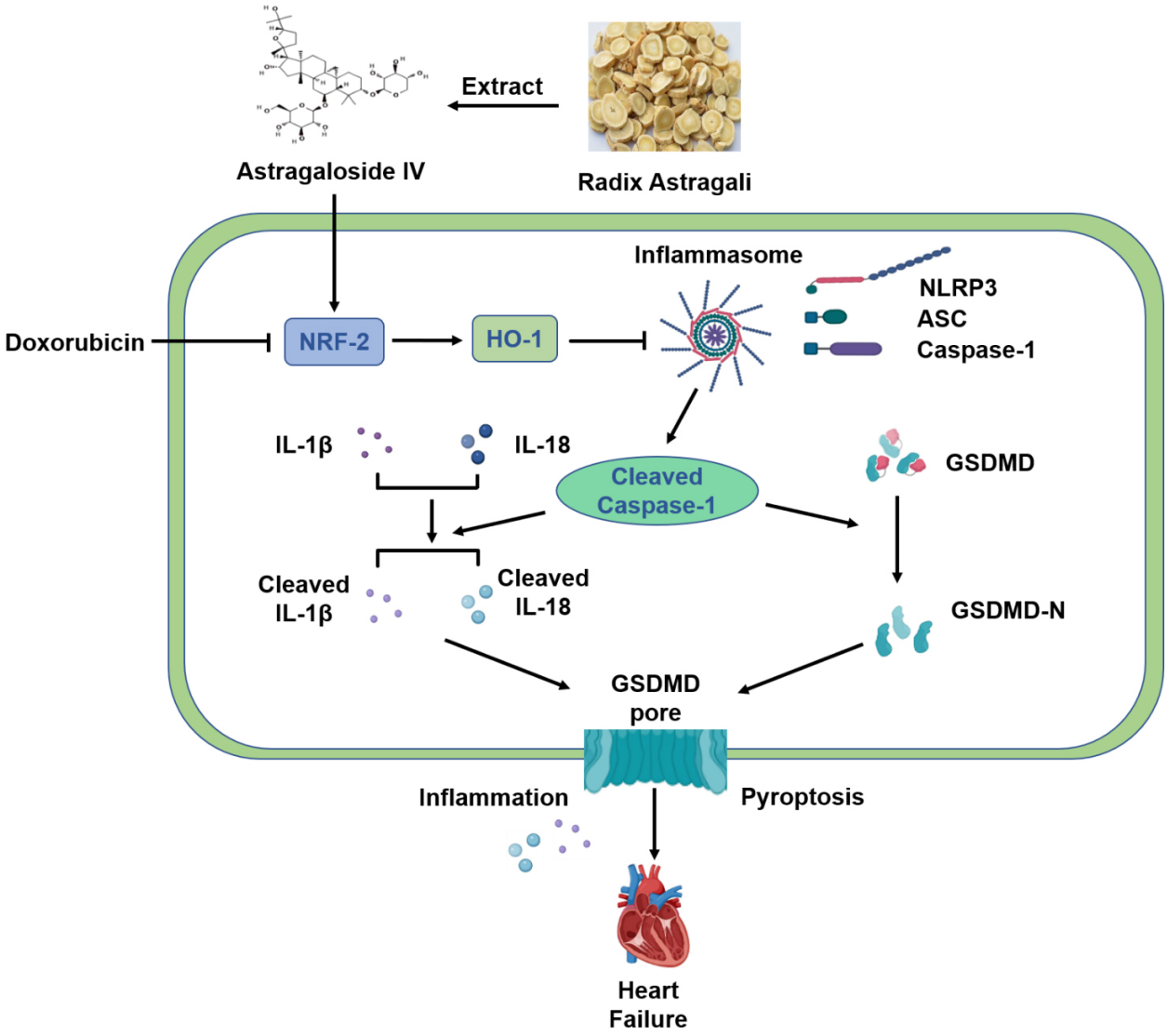

Fig. 7. Schematic diagram of protective mechanism of AS-IV against DOX-induced myocardial injury in mice. AS-IV is extracted from Radix astragali. DOX inhibits the expression of Nrf-2 and HO-1, which activates the assembly of NLRP3 inflammasome, leading to the cleavage of Caspase-1. Increased cleaved Caspase-1 then cleaves the inflammatory factors IL-1β and IL-18 to cleaved IL-1β and cleaved IL-18. GSDMD is also cleaved to GSDMD-N by cleaved Caspase-1, thus promoting the formations of cell membrane pores and pyroptosis. Moreover, inflammatory factors, including cleaved IL-1β and cleaved IL-18 then release to extracellular matrix. Both pyroptosis and inflammatory factors thus eventually lead to myocardial injury and cardiac dysfunction. AS-IV inhibits the pyroptosis by activating the Nrf-2/HO-1 pathway and exerts a cardioprotective effect on DOX-induced cardiac injuries.

found that AS-IV can promote Nrf-2/HO-1 signaling to reduce pressure overload-induced heart failure [27]. In this study, DOX reduced the expression of Nrf2, pNrf2 and HO-1, which was reversed by AS-IV treatment. Thus, we suggest that AS-IV ameliorates DOX-induced myocardial injury by inhibiting pyroptosis via activation of the Nrf-2/HO-1 pathway. However, other regulatory pathways for DOX-induced pyroptosis may exist; therefore, additional genetic modifications of mice or *in vitro* experiments are needed to verify the specific mechanism by which AS-IV inhibits DOX-induced cardiomyocyte pyroptosis.

5. Conclusions

In conclusion, our results suggest that AS-IV exerts a protective effect against DOX-induced myocardial injury by activating the Nrf-2/HO-1 signaling pathway and by inhibiting NLRP3-mediated pyroptosis (Fig. 7). These results provide evidence for AS-IV to be employed as a potential clinical therapeutic agent for mitigating DOX-induced cardiotoxicity. However, further research using positive controls or gene knockout mice will provide better evidences for verifying the specific mechanisms of the Nrf-2/HO-1 pathway in the protective role of AS-IV in suppressing DOX-induced pyroptosis.

Availability of Data and Materials

The datasets used and/or analyzed during the current study are available from the corresponding author on reasonable request.

Author Contributions

CS, JZ and XW conceived and designed this study. XC performed animal administration, echocardiographic examination, ELISA, and western blot data acquisition. CT and ZZ contributed to histological and immunofluorescent data acquisition. XC contributed to the figures and statistical analysis. XC wrote the manuscript. YQ, RM, XD and YZ conducted part of the western blot and data analysis. CS contributed to the revision of this manuscript. All authors contributed to editorial changes in the manuscript. All authors read and approved the final manuscript.

Ethics Approval and Consent to Participate

The experiments were conducted in accordance with the principles approved by the Animal Care and Use Committee of the Affiliated Hospital of Jining Medical University (Permission number: 2021C104). All animal procedures conformed to the US of Health Guidelines for the Care and Use of Laboratory Animals. All animals were carefully handled and euthanized during the study.

Acknowledgment

Not applicable.

Funding

This study was supported by Shandong Province Medical and health Science and Technology Development Program (2019WS364), the National Nature Science Foundation of China (No. 82000269), Jining City Science and Technology Key Research and Development Program (2018SMNS006), Research Fund for Academician Lin He New Medicine (JYHL2018FMS02) and Jining City Science and Technology Key Research and Development Program (2021YXNS069).

Conflict of Interest

The authors declare no conflict of interest.

Supplementary Material

Supplementary material associated with this article can be found, in the online version, at https://doi.org/10.31083/j.fbl2803045.

References

[1] Cagel M, Grotz E, Bernabeu E, Moretton MA, Chiappetta DA. Doxorubicin: nanotechnological overviews from bench to bedside. Drug Discovery Today. 2017; 22: 270–281.

[2] Shafei A, El-Bakly W, Sobhy A, Wagdy O, Reda A, Aboelenin O, *et al*. A review on the efficacy and toxicity of different doxorubicin nanoparticles for targeted therapy in metastatic breast cancer. Biomedicine Pharmacotherapy. 2017; 95: 1209–1218.

[3] Kim J, Shim MK, Cho Y, Jeon S, Moon Y, Choi J, *et al*. The safe and effective intraperitoneal chemotherapy with cathepsin B-specific doxorubicin prodrug nanoparticles in ovarian cancer with peritoneal carcinomatosis. Biomaterials. 2021; 279: 121189.

[4] Yan D, Wei H, Lai X, Ge Y, Xu S, Meng J, *et al*. Co-delivery of homoharringtonine and doxorubicin boosts therapeutic efficacy of refractory acute myeloid leukemia. Journal of Controlled Release. 2020; 327: 766–778.

[5] Mizutani H, Tada-Oikawa S, Hiraku Y, Kojima M, Kawanishi S. Mechanism of apoptosis induced by doxorubicin through the generation of hydrogen peroxide. Life Sciences. 2005; 76: 1439–1453.

[6] Corbett A, Osheroff N. When good enzymes go bad: Conversion of topoisomerase II to a cellular toxin by antineoplastic drugs. Chemical Research in Toxicology. 1993; 6: 585–597.

[7] Gewirtz D. A critical evaluation of the mechanisms of action proposed for the antitumor effects of the anthracycline antibiotics adriamycin and daunorubicin. Biochemical Pharmacology. 1999; 57: 727–741.

[8] Tavakoli Dargani Z, Singla R, Johnson T, Kukreja R, Singla DK. Exosomes derived from embryonic stem cells inhibit doxorubicin and inflammation-induced pyroptosis in muscle cells. Canadian Journal of Physiology and Pharmacology. 2018; 96: 304–307.

[9] Oliveira MS, Carvalho JL, Campos ACDA, Gomes DA, de Goes AM, Melo MM. Doxorubicin has in vivo toxicological effects on ex vivo cultured mesenchymal stem cells. Toxicology Letters. 2014; 224: 380–386.

[10] Bhagat A, Kleinerman ES. Anthracycline-Induced Cardiotoxicity: Causes, Mechanisms, and Prevention. Advances in Experimental Medicine and Biology. 2020; 26: 181–192.

[11] Dadson K, Calvillo-Argüelles O, Thavendiranathan P, Billia F. Anthracycline-induced cardiomyopathy: cellular and molecular mechanisms. Clinical Science. 2020; 134: 1859–1885.

[12] Kong C, Guo Z, Song P, Zhang X, Yuan Y, Teng T, *et al*. Underlying the Mechanisms of Doxorubicin-Induced Acute Cardiotoxicity: Oxidative Stress and Cell Death. International Journal of Biological Sciences. 2022; 18: 760–770.

[13] Zheng X, Zhong T, Ma Y, Wan X, Qin A, Yao B, *et al*. Bnip3 mediates doxorubicin-induced cardiomyocyte pyroptosis via caspase-3/GSDME. Life Sciences. 2020; 242: 117186.

[14] Man SM, Karki R, Kanneganti T. Molecular mechanisms and functions of pyroptosis, inflammatory caspases and inflammasomes in infectious diseases. Immunological Reviews. 2017; 277: 61–75.

[15] Zeng C, Wang R, Tan H. Role of Pyroptosis in Cardiovascular Diseases and its Therapeutic Implications. International Journal of Biological Sciences. 2019; 15: 1345–1357.

[16] Mariathasan S, Weiss DS, Newton K, McBride J, O'Rourke K, Roose-Girma M, *et al*. Cryopyrin activates the inflammasome in response to toxins and ATP. Nature. 2006; 440: 228–232.

[17] Zeng C, Duan F, Hu J, Luo B, Huang B, Lou X, *et al*. NLRP3 inflammasome-mediated pyroptosis contributes to the pathogenesis of non-ischemic dilated cardiomyopathy. Redox Biology. 2020; 34: 101523.

[18] Meng L, Lin H, Zhang J, Lin N, Sun Z, Gao F, *et al*. Doxorubicin induces cardiomyocyte pyroptosis via the TINCR-mediated posttranscriptional stabilization of NLR family pyrin domain containing 3. Journal of Molecular and Cellular Cardiology. 2019; 136: 15–26.

[19] Tavakoli Dargani Z, Singla DK. Embryonic stem cell-derived exosomes inhibit doxorubicin-induced TLR4-NLRP3-mediated cell death-pyroptosis. American Journal of Physiology-Heart and Circulatory Physiology. 2019; 317: H460–H471.

[20] Vejpongsa P, Yeh ETH. Prevention of Anthracycline-Induced Cardiotoxicity. Journal of the American College of Cardiology. 2014; 64: 938–945.
[21] Kim BM. The Role of Saikosaponins in Therapeutic Strategies for Age-Related Diseases. Oxidative Medicine and Cellular Longevity. 2018; 2018: 1–10.
[22] Lyu M, Wang Y, Fan G, Wang X, Xu S, Zhu Y. Balancing Herbal Medicine and Functional Food for Prevention and Treatment of Cardiometabolic Diseases through Modulating Gut Microbiota. Frontiers in Microbiology. 2017; 8: 2146.
[23] Su H, Shaker S, Kuang Y, Zhang M, Ye M, Qiao X. Phytochemistry and cardiovascular protective effects of Huang-Qi (Astragali Radix) Medicinal Research Reviews. 2021; 41: 1999–2038.
[24] Zhang J, Wu C, Gao L, Du G, Qin X. Astragaloside IV derived from Astragalus membranaceus: a research review on the pharmacological effects. Pharmacological Advances in Natural Product Drug Discovery. 2020; 10: 89–112.
[25] Dong Z, Zhao P, Xu M, Zhang C, Guo W, Chen H, *et al*. Astragaloside IV alleviates heart failure via activating PPARα to switch glycolysis to fatty acid β-oxidation. Scientific Reports. 2017; 7: 2691.
[26] Tu L, Pan C, Wei X, Yan L, Liu Y, Fan J, *et al*. Astragaloside IV protects heart from ischemia and reperfusion injury via energy regulation mechanism. Microcirculation. 2013; 20: 736–747.
[27] Nie P, Meng F, Zhang J, Wei X, Shen C. Astragaloside IV Exerts a Myocardial Protective Effect against Cardiac Hypertrophy in Rats, Partially via Activating the Nrf2/HO-1 Signaling Pathway. Oxidative Medicine and Cellular Longevity. 2019; 2019: 1–16.
[28] Wei Y, Wu Y, Feng K, Zhao Y, Tao R, Xu H, *et al*. Astragaloside IV inhibits cardiac fibrosis via miR-135a-TRPM7-TGF-β/Smads pathway. Journal of Ethnopharmacology. 2020; 249: 112404.
[29] Wang Q, Yang X, Song Y, Sun X, Li W, Zhang L, *et al*. Astragaloside IV-targeting miRNA-1 attenuates lipopolysaccharide-induced cardiac dysfunction in rats through inhibition of apoptosis and autophagy. Life Sciences. 2021; 275: 119414.
[30] Yu W, Qin X, Zhang Y, Qiu P, Wang L, Zha W, *et al*. Curcumin suppresses doxorubicin-induced cardiomyocyte pyroptosis via a PI3K/Akt/mTOR-dependent manner. Cardiovascular Diagnosis and Therapy. 2020; 10: 752–769.
[31] Lin J, Fang L, Li H, Li Z, Lyu L, Wang H, *et al*. Astragaloside IV alleviates doxorubicin induced cardiomyopathy by inhibiting NADPH oxidase derived oxidative stress. European Journal of Pharmacology. 2019; 859: 172490.
[32] Li C, Song H, Chen C, Chen S, Zhang Q, Liu D, *et al*. LncRNA PVT1 Knockdown Ameliorates Myocardial Ischemia Reperfusion Damage via Suppressing Gasdermin D-Mediated Pyroptosis in Cardiomyocytes. Frontiers in Cardiovascular Medicine. 2021; 8: 747802.
[33] Wang J, Deng B, Liu Q, Huang Y, Chen W, Li J, *et al*. Pyroptosis and ferroptosis induced by mixed lineage kinase 3 (MLK3) signaling in cardiomyocytes are essential for myocardial fibrosis in response to pressure overload. Cell Death & Disease. 2020; 11: 574.
[34] Zheng D, Liu J, Piao H, Zhu Z, Wei R, Liu K. ROS-triggered endothelial cell death mechanisms: Focus on pyroptosis, parthanatos, and ferroptosis. Frontiers in Immunology. 2022; 13: 1039241.
[35] Cheng L, Zhang W. DJ-1 affects oxidative stress and pyroptosis in hippocampal neurons of Alzheimer's disease mouse model by regulating the Nrf2 pathway. Experimental and Therapeutic Medicine. 2021; 21: 557.
[36] Li J, Zhao C, Zhu Q, Wang Y, Li G, Li X, *et al*. Sweroside Protects Against Myocardial Ischemia-Reperfusion Injury by Inhibiting Oxidative Stress and Pyroptosis Partially via Modulation of the Keap1/Nrf2 Axis. Frontiers in Cardiovascular Medicine. 2021; 8: 650368.
[37] Hu Q, Zhang T, Yi L, Zhou X, Mi M. Dihydromyricetin inhibits NLRP3 inflammasome-dependent pyroptosis by activating the Nrf2 signaling pathway in vascular endothelial cells. BioFactors. 2018; 44: 123–136.
[38] Chen Y, Tang Y, Xiang Y, Xie Y, Huang X, Zhang Y. Shengmai Injection Improved Doxorubicin-Induced Cardiomyopathy by Alleviating Myocardial Endoplasmic Reticulum Stress and Caspase-12 Dependent Apoptosis. BioMed Research International. 2015; 2015: 1–8.
[39] Zhang X, Hu C, Kong C, Song P, Wu H, Xu S, *et al*. FNDC5 alleviates oxidative stress and cardiomyocyte apoptosis in doxorubicin-induced cardiotoxicity via activating AKT. Cell Death Differentiation. 2020; 27: 540–555.
[40] Li X, Liu Y, Yi J, Dong J, Zhang P, Wan L, *et al*. MicroRNA-143 Increases Oxidative Stress and Myocardial Cell Apoptosis in a Mouse Model of Doxorubicin-Induced Cardiac Toxicity. Medical Science Monitor: International Medical Journal of Experimental and Clinical Research. 2020; 26: e920394.
[41] Cengiz O, Baran M, Balcioglu E, Suna PA, Bilgici P, Goktepe O, *et al*. Use of selenium to ameliorate doxorubicin induced hepatotoxicity by targeting pro-inflammatory cytokines. Biotechnic Histochemistry. 2021; 96: 67–75.
[42] Jo C, Kim S, Park J, Kim G. Anti-Inflammatory Action of Sitagliptin and Linagliptin in Doxorubicin Nephropathy. Kidney and Blood Pressure Research. 2018; 43: 987–999.
[43] Xue Y, Enosi Tuipulotu D, Tan WH, Kay C, Man SM. Emerging Activators and Regulators of Inflammasomes and Pyroptosis. Trends in Immunology. 2019; 40: 1035–1052.
[44] Wang X, Lian Z, Ge Y, Yu D, Li S, Tan K. TRIM25 Rescues against Doxorubicin-Induced Pyroptosis through Promoting NLRP1 Ubiquitination. Cardiovascular Toxicology. 2021; 21: 859–868.
[45] Maayah ZH, Alam AS, Takahara S, Soni S, Ferdaoussi M, Matsumura N, *et al*. Resveratrol reduces cardiac NLRP3-inflammasome activation and systemic inflammation to lessen doxorubicin-induced cardiotoxicity in juvenile mice. FEBS Letters. 2021; 595: 1681–1695.
[46] Zhang C, Yang X, Wei J, Chen N, Xu J, Bi Y, *et al*. Ethnopharmacology, Phytochemistry, Pharmacology, Toxicology and Clinical Applications of Radix Astragali. Chinese Journal of Integrative Medicine. 2021; 27: 229–240.
[47] Fu S, Zhang J, Menniti-Ippolito F, Gao X, Galeotti F, Massari M, *et al*. Huangqi injection (a traditional Chinese patent medicine) for chronic heart failure: a systematic review. PLoS ONE. 2011; 6: e19604.
[48] Lu S, Chen K, Yang Q, Sun H. Progress in the research of Radix Astragali in treating chronic heart failure: Effective ingredients, dose-effect relationship and adverse reaction. Chinese Journal of Integrative Medicine. 2011; 17: 473–477.
[49] Tsao SM, Wu TC, Chen J, Chang F, Tsao T. Astragalus Polysaccharide Injection (PG2) Normalizes the Neutrophil-to-Lymphocyte Ratio in Patients with Advanced Lung Cancer Receiving Immunotherapy. Integrative Cancer Therapies. 2021; 20: 153473542199525.
[50] Guo L, Bai S, Zhao L, Wang X. Astragalus polysaccharide injection integrated with vinorelbine and cisplatin for patients with advanced non-small cell lung cancer: effects on quality of life and survival. Medical Oncology. 2012; 29: 1656–1662.
[51] Monschein M, Ardjomand-Woelkart K, Rieder J, Wolf I, Heydel B, Kunert O, *et al*. Accelerated sample preparation and formation of astragaloside IV in Astragali Radix. Pharmaceutical Biology. 2014; 52: 403–409.
[52] Lin X, Wang Q, Sun S, Xu G, Wu Q, Qi M, *et al*. Astragaloside IV promotes the eNOS/no/cGMP pathway and improves left ventricular diastolic function in rats with metabolic syn-

drome. Journal of International Medical Research. 2020; 48: 030006051982684.
[53] Sun C, Zeng G, Wang T, Ren H, An H, Lian C, *et al*. Astragaloside IV Ameliorates Myocardial Infarction Induced Apoptosis and Restores Cardiac Function. Frontiers in Cell and Developmental Biology. 2021; 9: 671255.
[54] Nie Q, Zhu L, Zhang L, Leng B, Wang H. Astragaloside IV protects against hyperglycemia-induced vascular endothelial dysfunction by inhibiting oxidative stress and Calpain-1 activation. Life Sciences. 2019; 232: 116662.
[55] Xu C, Tang F, Lu M, Yang J, Han R, Mei M, *et al*. Astragaloside IV improves the isoproterenol-induced vascular dysfunction via attenuating eNOS uncoupling-mediated oxidative stress and inhibiting ROS-NF-κB pathways. International Immunopharmacology. 2016; 33: 119–127.
[56] Huang D, Shi S, Wang Y, Wang X, Shen Z, Wang M, *et al*. Astragaloside IV alleviates PM2.5-caused lung toxicity by inhibiting inflammasome-mediated pyroptosis via NLRP3/caspase-1 axis inhibition in mice. Biomedicine Pharmacotherapy. 2022; 150: 112978.
[57] Xiao L, Dai Z, Tang W, Liu C, Tang B. Astragaloside IV Alleviates Cerebral Ischemia-Reperfusion Injury through NLRP3 Inflammasome-Mediated Pyroptosis Inhibition via Activating Nrf2. Oxidative Medicine and Cellular Longevity. 2021; 2021: 1–14.
[58] Tang B, She X, Deng C. Effect of the combination of astragaloside IV and saponins on pyroptosis and necroptosis in rat models of cerebral ischemia-reperfusion. Experimental and Therapeutic Medicine. 2021; 22: 1123.
[59] Heid ME, Keyel PA, Kamga C, Shiva S, Watkins SC, Salter RD. Mitochondrial Reactive Oxygen Species Induces NLRP3-Dependent Lysosomal Damage and Inflammasome Activation. Journal of Immunology. 2013; 191: 5230–5238.
[60] Lupfer C, Anand P, Liu Z, Stokes K, Vogel P, Lamkanfi M, *et al*. Reactive oxygen species regulate caspase-11 expression and activation of the non-canonical NLRP3 inflammasome during enteric pathogen infection. PLoS Pathogens. 2014; 10: e1004410.
[61] Zhang M, Jiang Y, Yang Y, Liu J, Huo C, Ji X, *et al*. Cigarette smoke extract induces pyroptosis in human bronchial epithelial cells through the ROS/NLRP3/caspase-1 pathway. Life Sciences. 2021; 269: 119090.
[62] Tonelli C, Chio IIC, Tuveson DA. Transcriptional Regulation by Nrf2. Antioxidants Redox Signaling. 2018; 29: 1727–1745.
[63] Liu X, Zhang X, Ding Y, Zhou W, Tao L, Lu P, *et al*. Nuclear Factor E2-Related Factor-2 Negatively Regulates NLRP3 Inflammasome Activity by Inhibiting Reactive Oxygen Species-Induced NLRP3 Priming. Antioxidants Redox Signaling. 2017; 26: 28–43.
[64] Zhu C, Zhao Y, Wu X, Qiang C, Liu J, Shi J, *et al*. The therapeutic role of baicalein in combating experimental periodontitis with diabetes via Nrf2 antioxidant signaling pathway. Journal of Periodontal Research. 2020; 55: 381–391.
[65] Wunder C, Potter R. The Heme Oxygenase System: its Role in Liver Inflammation. Current Drug Target -Cardiovascular Hematological Disorders. 2003; 3: 199–208.
[66] Lin Y, Luo T, Weng A, Huang X, Yao Y, Fu Z, *et al*. Gallic Acid Alleviates Gouty Arthritis by Inhibiting NLRP3 Inflammasome Activation and Pyroptosis Through Enhancing Nrf2 Signaling. Frontiers in Immunology. 2020; 11: 580593.